Scientific paper

The Paramagnetic or Spin Crossover Iron(III) Complexes Based-on Pentadentate Schiff Base Ligand: Crystal Structure, and Magnetic Property Investigation

Zhijie Xu, Shuo Meng, Tong Cao, Yu Xin, Mingjian Zhang, Xiaoyi Duan, Zhen Zhou and Daopeng Zhang*

College of Chemical and Chemical Engineering, Shandong University of Technology, Zibo 255049, PR China

** Corresponding author: E-mail: dpzhang73@126.com*

Received: 07-12-2022

Abstract

A series of bi- or mononuclear hexacoordinate iron(III) complexes, $[Fe(L)][Fe(bpb)(CN)_2]\cdot\mathbf{CH}_3OH\cdot0.5H_2O$ (**1**), $[Fe(L)][Co(bpb)(CN)_2]\cdot\mathbf{CH}_3OH$ (**2**) $[(Fe(L))_2(4,4'\text{-bipy})](BPh_4)_2$ (**3**), $[Fe(L)(py)](BPh_4)$ (**4**) and $[Fe(L)(dmap)](BPh_4)$ (**5**) (bpb = 1,2-bis(pyridine-2-carboxamido)benzenate, L = *N*,*N*'-bis(2-hydroxybenzyliden)-1,7-diamino-4-azaheptane, dmap = 4-dimethylaminopyridine), have been prepared with the pentadentate Schiff base iron(III) compound as assemble precursor and characterized by element analysis, IR and X-ray diffraction. Single crystal structural determination revealed the neutral cyanide-bridged binuclear entity for complexes **1** and **2** and the cationic di- or mononuclear structure for complexes **3**–**5** with the positive charge(s) balanced by BPh_4^- ion(s). The experimental study and theoretical simulation of the magnetic property discovered the ferromagnetic coupling between the Fe(III) ions bridged by cyanide group in complex **1** and the always high spin state of the Fe(III) ion coordinated to the Schiff base ligand in both complexes **1** and **2**. The temperature dependent magnetic susceptibility investigation over complexes **3**–**5** showed the occurrence of the thermo-induced gradual complete spin crossover (SCO) property at about 115, 170 and 200 K, respectively.

Keywords: Cyanide-bridged, Crystal structure, Ferromagnetic coupling, Spin crossover

Introduction

Since the 21st century, the synthesis of materials with special functions and applications based on the coordination chemistry has been one of the important directions of current chemical research.[1–10] Molecular materials with spin crossover behavior have broad application prospects in the fields of nano device, spintronics, information storage, sensors, digital display, and so on.[11–18] The use of spin crossover complexes as switches or sensors depent on spin transition distinguished by different magnetic, optical and structural characteristics, which included structural changes between two different spin states and could be realized under the suitable coordination field by external stimuli such as temperature, light irradiation and the guest solvent molecules.[19–25] It was generally found that the metal centers with the $3d^4$–$3d^7$ electronic configurations and involved in octahedral coordination surroundings could readily occur spin transition between the different spin states.[26–28]

Among $3d^4$–$3d^7$ metal ions, the strong interest has always been devoted to the switchable molecular materials centered with iron(II) ion. During the past several decades, a great deal of the Fe(II)-based complexes with various structure types from 0D clusters, 1D infinite chains to 2–3D networks and interesting SCO properties have been reported. However, with comparison to the intensely studied divalent Fe(II) in SCO field, research on Fe(III) ion-based SCO material is comparatively limited,[29–33] as is also with the SCO possibility between the high spin S = 5/2 and low spin S = 1/2. The pentadentate Schiff base ligands (Scheme 1), which can encapsulate the hexa-coordinated metal with sixth position weakly bonded to other ligand, are a type of precursor for preparation function complexes.[34–36] In fact, some previous reports have proven that the above pentadentate Schiff base based iron(III) compounds are suitable candidates for assembling SCO materials under the help of the pyridine-like ligands[37,38] and some of the obtained complexes have been structurally characterized and experimentally magnetic investigated. Taking into account that the cyanometallic precursors with tunable coordination field, such as $[M(CN)_4]^{2-}$ (M = Ni, Pd,

Pt), $[M'(CN)_2]^-$ (M' = Cu, Ag, Au) and other polycyanometallates, have been widely employed to construct SCO materials, especially for those ones with Hoffman topologic structures,[39–42] the reactions of the pentadentate Schiff base iron(III) compound with the *trans*-dicyanoiron(III)/cobalt(III) building blocks (Scheme 1), for the latter which has been extensively used to prepare cyanide-bridged molecular magnetic materials by our group,[43–46] were investigated, resulting in two new binuclear homo- or heterometallic complexes formulated as $[Fe(L)][Fe(bpb)(CN)_2]$ CH_3OH $0.5H_2O$ (**1**), $[Fe(L)][Co(bpb)(CN)_2]$ CH_3OH (**2**) (bpb = 1,2-bis(pyridine-2-carboxamido)benzenate, L = saldptn = N,N'-bis(2-hydroxybenzyliden)-1,7-diamino-4-azaheptane).[47,48] At the same time, by using 4,4'-bipy,[49] py or dmap (dmap = 4-dimethylaminopyridine) as ancillary ligand, three monometallic Fe(III) complexes with the formula $[(Fe(L))_2(4,4'\text{-bipy})](BPh_4)_2$ (**3**), $[Fe(L)(py)](BPh_4)$ (**4**) and $[Fe(L)(dmap)](BPh_4)$ (**5**) have been successfully obtained. The synthesis, crystal structures and magnetic properties for the reported complexes will be detailed described in this paper.

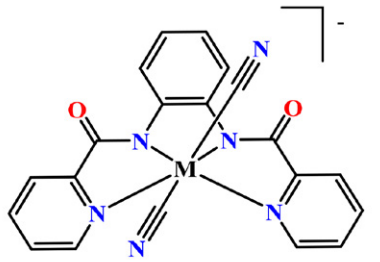

trans-$[M^{III}(bpb)(CN)_2]^-$ (M = Fe, Co)

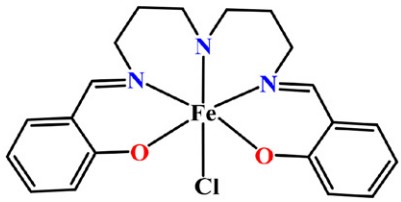

[Fe(saldptn)]Cl

Scheme 1. Structure of the Schiff base iron(III) precursor and the *trans*-dicyano building blocks.

2. Experimental Section

Elemental analyses (C, H and N) were carried out with a VarioEl element analyser. IR spectroscopic analysis on KBr pellets was performed on a Magna-IR 750 spectrophotometer in the 4000–400 cm^{-1} region. Variable-temperature magnetic susceptibility and field-dependent magnetization measurements were performed on a Quantum Design MPMS SQUID magnetometer. The experimental susceptibilities were corrected for the diamagnetism of the constituent atoms (Pascal'stables).

General procedures and materials. All the reactions were carried out under air atmosphere and all chemicals and solvents used were reagent grade without further purification. H_2L, $[Fe(L)]Cl$, $K[Fe(bpb)(CN)_2]$ and $K[Co(bpb)(CN)_2]$ were prepared to accord to experimental methods already described.[50–52]

Caution! KCN is hypertoxic and should be handled in small quantities with great care.

2. 1. The Preparation of the Complexes 1 and 2

A solution containing $K[Fe(bpb)(CN)_2]$ (0.10 mmol, 46.5 mg) or $K[Co(bpb)(CN)_2]$ (0.10 mmol, 46.7 mg) dissolved in methanol (10 mL) was slowly added into the methanol-water (10 mL, 4:1 v/v) solution of $[Fe(L)]Cl$ (43 mg, 0.10 mmol) under the stirring. The mixture was stirred at room temperature for several minutes and filtered to remove any insoluble substances. Then, the filtrate was allowed for slow evaporation without interference for about two weeks. Dark brown crystals suitable for X-ray diffraction were collected by filtration, washed with cold methanol and dried in air.

Complex **1**: Yield: 52.9 mg, 61.7%. Anal. Calcd. For $C_{41}H_{40}Fe_2N_9O_5$: C, 57.36; H, 4.70; N, 14.68. Found: C, 57.47; H, 4.62; N, 14.79. Main IR bands (cm^{-1}): 2160, 2120 (s, νC–N), 1630 (vs νC=N), 3056, 2846, 2660 (w, νC–H), 1444, 1401, 1279 (s, νC–O).

Complex **2**: Yield 53.9 mg, 63.3%. Anal. Calcd. For $C_{41}H_{39}CoFeN_9O_5$: C, 57.76; H, 4.61; N, 14.79. Found: C, 57.87; H, 4.52; N, 14.89. Main IR bands (cm^{-1}): 2158, 2122 (s, νC–N), 1630 (vs νC=N), 3059, 2855, 2656 (w, νC–H), 1458, 1387, 1275 (s, νC–O).

2. 2. The Preparation of Complexes 3–5

To a methanol solution of $[Fe(L)]Cl$ (43 mg, 0.10 mmol) was added 4,4'-bipy(7 mg, 0.05 mmol) or py (8 mg, 0.1 mmol) or dmap (12 mg, 0.1 mmol). The mixture was stirred for about ten minutes at 60 °C before an excess of sodium tetraphenylborate (855 mg, 2.5 mmol) was added. After the insoluble substances were filtered out, the filtrate was partial evaporated and the crystals obtained was collected and washed with methanol and ether.

Complex **3**: Yield 48.0 mg, 60.7 %. Anal. Calcd. for $C_{98}H_{94}B_2Fe_2N_8O_4$: C, 74.44; H, 5.99; N, 7.09. Found: C, 74.52; H, 5.93; N, 7.15. Main IR bands (cm^{-1}): 1633 (vs **νC**=N), 732, 708 (νB–C), 3057, 2978 (w, νC–H), 1251 (s, νC–O). Anal.

Complex **4**: Yield 42.0 mg, 53.1 %. Anal. Calcd. for $C_{49}H_{48}BFeN_4O_2$: C, 74.34; H, 6.11; N, 7.08. Found: C, 74.44; H, 6.01; N, 7.15. Main IR bands (cm^{-1}): 1628 (vs νC=N), 735, 706 (νB–C), 3054, 2977 (w, νC–H), 1252 (s, νC–O). Anal.

Complex **5**: Yield 42.6 mg, 51.2 %. Anal. Calcd. for $C_{51}H_{52}BFeN_5O_2$: C, 73.48; H, 6.29; N, 8.40. Found: C, 73.54; H, 6.19; N, 8.54. Main IR bands (cm^{-1}): 1630 (vs **νC**=N), 733, 707 (νB–C), 3050, 2975 (w, νC–H), 1245 (s, νC–O). Anal.

2. 3. X-ray Data Collection and Structure Refinement

Single crystals of all the complexes for X-ray diffraction analyses with suitable dimensions were mounted on a glass rod and the crystal data were collected on a Bruker SMART CCD diffractometer with a Mo Kα sealed tube (λ = 0.71073 Å) at 293 K, using a ω scan mode. For complexes **3** and **4**, their structures have been further measured at about 120 K. The structures were solved by direct methods and expanded to use Fourier difference techniques with the SHELXTL-97 program package. The non-hydrogen atoms were refined anisotropically, while hydrogens were introduced as fixed contributors. All non-hydrogen atoms were refined with anisotropic displacement coefficients. Hydrogens were assigned isotropic displacement coefficients U(H) = 1.2U(C) or 1.5U(C), and their coordinates were allowed riding on their respective carbons using SHELXL-2018, except some hydrogens of solvent molecules, which were refined isotropically with fixed U values and the DFIX command was used to rationalize the bond parameters. CCDC 2169018–2169022 for complexes **1**–**5** contain the supplementary crystallographic data for this paper. These data can be obtained free of charge from the Cambridge Crystallographic Data Centre via www.ccdc.cam.ac.uk/data_request/cif.Details of the crystal parameters, data collection, and refinement are summarized in tables **1** and **2**.

Table 1. Crystallographic data for complexes **1, 2** and **5**.

	1 (293k)	**2 (293k)**	**5 (293k)**
Chemical formula	$C_{41}H_{40}Fe_2N_9O_{5.5}$	$C_{41}H_{39}CoFeN_9O_5$	$C_{51}H_{53}BFeN_5O_2$
Fw	858.52	852.59	834.64
Crystal system	Monoclinic	Monoclinic	Monoclinic
Space group	$P2_1/c$	$P2_1$	$P2_1/n$
a/Å	10.8753(10)	10.875(7)	18.3588(16)
b/Å	10.0446(9)	10.065(6)	14.5766(13)
c/Å	36.595(3)	18.331(11)	18.5738(16)
α/deg	90.0	90.0	90
β/deg	92.349(2)	95.586(11)	117.698(2)
γ/deg	90.0	90.0	90
Z	2	2	4
V/Å^3	3994.2(6)	1997(2)	4400.9(7)
F(000)	1780.0	882.0	1764.0
GOF	1.030	1.028	1.024
R_1 [I >2σ(I)]	0.1241	0.073	0.1180
wR_2 (all data)	0.1435	0.1901	0.1455

Table 2. Crystallographic data for complexes **3** and **4**.

	3 (293k)	**3 (120k)**	**4 (293k)**	**4 (120k)**
Chemical formula	$C_{49}H_{48}BFeN_4O_2$	$C_{49}H_{48}BFeN_4O_2$	$C_{98}H_{94}B_2Fe_2N_8O_4$	$C_{98}H_{94}B_2Fe_2N_8O_4$
Fw	791.57	791.57	1581.13	1581.13
Crystal system	Monoclinic	Monoclinic	Monoclinic	Monoclinic
Space group	$P2_1/c$	$P2_1/c$	C2/c	C2/c
a/Å	18.373(2)	18.295(4)	33.480(2)	33.1757(16)
b/Å	11.9535(13)	11.880(2)	16.7773(11)	16.7010(6)
c/Å	21.064(2)	20.678(4)	16.3933(11)	16.0077(6)
α/deg	90.0	90.0	90.0	90.0
β/deg	114.530(2)	114.60(3)	117.094(1)	116.567(5)
γ/deg	90.0	90.0	90.0	90.0
Z	4	4	4	4
V/Å^3	4208.6(8)	4086.5(4)	8197.6(10)	7932.9(6)
F(000)	1668.0	1668.0	3328.0	3328.0
GOF	1.006	1.028	1.005	1.027
R_1 [I >2σ(I)]	0.0415	0.0462	0.1159	0.0607
wR_2 (all data)	0.1086	0.0793	0.1394	0.1503

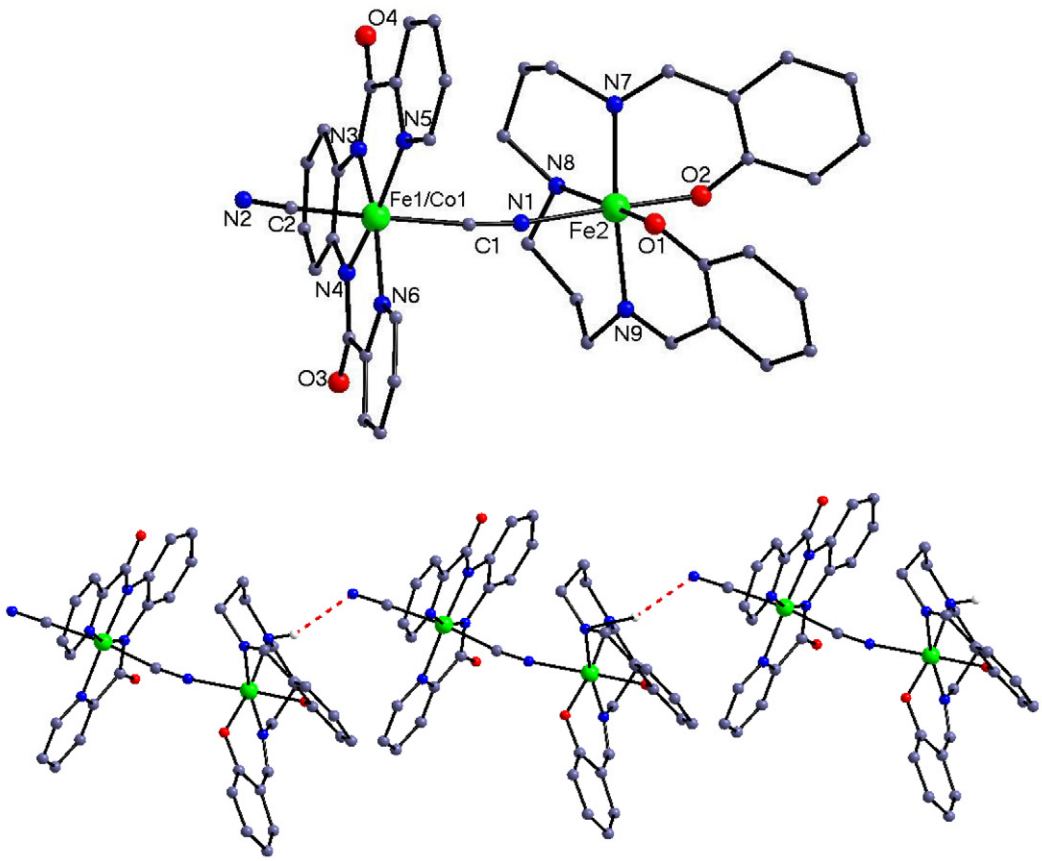

Figure 1. The neutral binuclear structures of complexes **1** and **2** (top) and the 1D supramolecular chain constructed by H-bond interactions (bottom). All the H atoms except one used to form H-bond and the solvent content have been omitted for clarity.

3 Results and Discussion

3. 1. Crystal Structure Description

3. 1. 1 Crystal Structures of Complexes 1 and 2

The selected important structural parameters for complexes **1** and **2** are collected in Table 3. The neutral binuclear and the 1D supramolecular single chain structure constructed by the hydrogen bond interactions for these two complexes are shown in Figure 1.

The structures of complexes **1** and **2**, crystallizing in space group $P2_1/c$ and $P2_1$ containing four and two independent units in the unit cell, respectively, belong to neutral binuclear entity. The $[Fe/Co(bpb)(CN)_2]^-$ anion acting as monodentate ligand connects the $[Fe(L)]^+$ cation through one cyanide group with the other *trans* one terminal, therefore forming neutral binuclear dimer. The Fe^{III}/Co^{III} in the cyano precursors with low spin state is coordinated by an equatorial N_4 unit from bpb and two carbons of cyanide groups in the *trans* position. The Fe^{III}/Co^{III}–N bond lengths were slightly longer than the Fe^{III}/Co^{III}–$C_{cyanide}$ ones (1.923(8)–1.976(5) Å), revealing a slightly distorted octahedral geometry around the metal ions. As listed in Table 3, the bond angles of Fe^{III}/Co^{III}–C–N very close to

Table 3. Selected bond lengths (Å) and angles (°) for complexes **1** and **2**.

Complexes	Fe	Co1
Fe2–O1	1.911(3)	1.918(5)
Fe2–O2	1.927(3)	1.900(5)
Fe2–N1	2.134(4)	2.141(7)
Fe2–N7	2.098(4)	2.087(7)
Fe2–N8	2.201(4)	2.202(7)
Fe2–N9	2.108(4)	2.115(8)
Fe1/Co1–C1	1.976(5)	1.923(8)
Fe1/Co1–C2	1.951(5)	1.893(8)
Fe1/Co1–N3	1.879(4)	1.894(6)
Fe1/Co1–N4	1.891(4)	1.885(6)
Fe1/Co1–N5	1.933(4)	1.960(5)
Fe1/Co1–N6	2.004(4)	1.963(6)
C1–Fe1/Co1–N6	90.56(16)	88.0(3)
O1–Fe2–N9	89.66(14)	95.1(3)
N1–C1–Fe1/Co1	172.5(4)	173.9(6)
C2–Fe1/Co1–C1	168.93(19)	174.3(3)
O2–Fe2–N1	179.01(15)	179.2(3)
N2–C2–Fe1/Co1	175.2(5)	174.1(7)
N3–Fe1/Co1–N4	83.26(19)	82.4(3)
N4–Fe1/Co1–C1	91.47(11)	90.0(3)

180° clearly indicated that the three atoms were with prefect linear conformation.

The coordination sphere of Fe^{III} ion in $[Fe(L)]^+$ is six-coordinated octahedron, in which the four equatorial positions are occupied by three N atoms and one O atom from the Schiff base ligand and the two axial ones coordinated by one O atom of the Schiff base ligand and one N atom of the bridge cyanide group. The averaged $Fe–N_{cyanide}$ and $Fe–N_{Schiff\ base}$ bond lengths in complexes **1** and **2** are 2.134(4), 2.141(7), 2.136(4) and 2.147(7) Å, respectively, longer than the averaged $Fe–O_{Schiff\ base}$ bond with the values of 1.919(3) and 1.909(5) Å, demonstrating the obviously distorted octahedral geometry around the Fe(III) ion in $[Fe(L)]^+$ unit. These bond lengths are in good agreement with the corresponding bond lengths around the high spin Fe(III) ion found in the reported complexes,[53] indicative of the high spin state of Fe(III) ions involved in the Schiff base precursor in these two complexes. Different from the perfect linear $Fe^{III}/Co^{III}–C–N$ unit, the $C–N–Fe^{II}/Co^{III}$ bond angles are some bent with the values of 172.2(5) and 169.7(6)°, respectively. With the help of the intermolecular N–H···N hydrogen bond interactions, the binuclear entity can be further constructed into supramolecular 1D infinite structure.

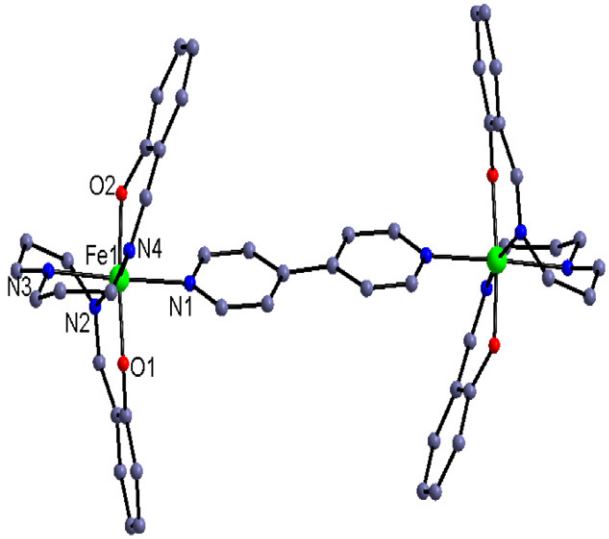

Figure 2. The cationic binuclear structure of complex **3**. All the H atoms and the balanced anions have been omitted for clarity.

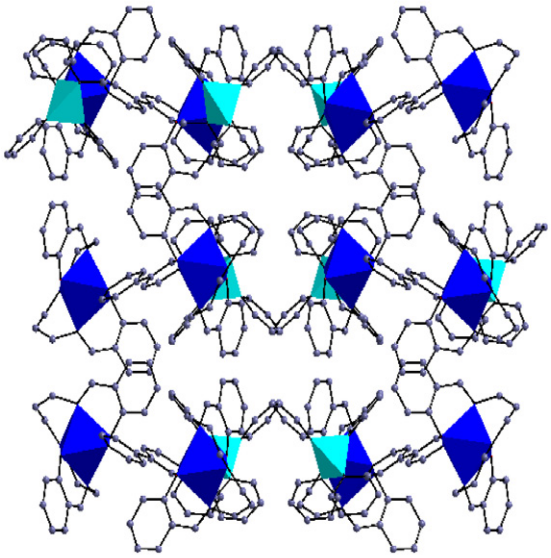

Figure 3. The cell packing diagram of complex **3** along b axial. All the H atoms have been omitted for clarity.

3. 1. 2 Crystal Structures of Complexes 3–5

Some important bond parameters for complexes **3–5** are given in Table 4. The cationic bi- or mononuclear

Table 4. Selected bond lengths (Å) and angles (°) for complexes **3–5** at room and low temperature

Complex 3	**(293K)**	**(120K)**
Fe1–O1	1.889(5)	1.8725(5)
Fe1–O2	1.895(5)	1.8827(5)
Fe1–N1	2.094(7)	2.012(7)
Fe1–N2	1.999(7)	1.952(7)
Fe1–N3	2.083(6)	2.01(6)
Fe1–N4	2.007(6)	1.961(6)
O1–Fe1–N1	88.34(9)	87.42(11)
O1–Fe1–O2	174.20(10)	175.91(11)
O2–Fe1–N2	92.72(11)	87.87(13)
O2–Fe1–N3	91.66(11)	93.16(12)
O2–Fe1–N4	88.58(12)	91.57(13)
N2–Fe1–N4	168.15(12)	173.79(13)
N3–Fe1–N1	177.43(10)	178.29(13)
Complex 4	**(293K)**	**(120K)**
Fe1–O1	1.889(5)	1.8725(17)
Fe1–O2	1.895(5)	1.8827(18)
Fe1–N1	2.094(7)	2.012(2)
Fe1–N2	1.999(7)	1.961(2)
Fe1–N3	2.083(6)	2.020(2)
Fe1–N4	2.007(6)	1.952(2)
O1–Fe1–N1	88.2(3)	88.77(8)
O2–Fe1–O1	175.3(2)	176.04(8)
O2–Fe1–N2	92.2(3)	91.26(8)
O2–Fe1–N3	90.7(2)	90.53(8)
O2–Fe1–N4	89.3(2)	89.47(8)
N3–Fe1–N1	177.6(3)	177.42(9)
N4–Fe1–N1	94.3(3)	91.27(8)

Complex 5 (293K)			
Fe1–O1	1.883(2)	Fe1–O2	1.901(2)
Fe1–N1	2.011(3)	Fe1–N3	1.996(3)
Fe1–N4	2.060(4)	Fe1–N5	1.985(3)
O1–Fe1–N1	92.09(11)	O1–Fe1–N5	90.63(12)
O1–Fe1–O2	179.06	N1–Fe1–N4	179.95(19)
O2–Fe1–N3	91.31(12)	O2–Fe1–N4	91.30(13)
N3–Fe1–N1	91.52(12)	N3–Fe1–N5	176.01(13)
C24–N4–Fe1	116.8(4)	C25–N4–Fe1	117.6(4)

structures are presented in Figure 2 and the cell packing diagram with complex **3** as representative is shown in Figure 3. As can be found, the three complexes, which crystallizes in *C*2/*c*, $P2_1/c$ and $P2_1/n$ space group, respectively, are composed by cationic bi- or mononuclear entity and the balanced BPh_4^- anion(s). For complex **3**, the asymmetric unit contains only half the dinuclear molecule. In complexes **3**–**5**, the coordination geometry of the Fe(III) ion is octahedron, in which the equatorial plane is connected by the N_2O_2 unit from the Schiff base ligand, different from that in complexes **1** and **2**, and the two axial positions are occupied by the N atom of the Schiff base ligand and the N atom of the pyridine ligand. It should be pointed out that the configuration of the Schiff base ligand in these three complexes are obviously different from that in complexes **1** and **2**, implying maybe the different spin state of the Fe(III) ion. Additionally, there exist weak π-π stacking interactions in complex **3** between the pyridine ring and the benzene ring of the BPh_4^- with center-center distance of 3.74(7) **Å**.

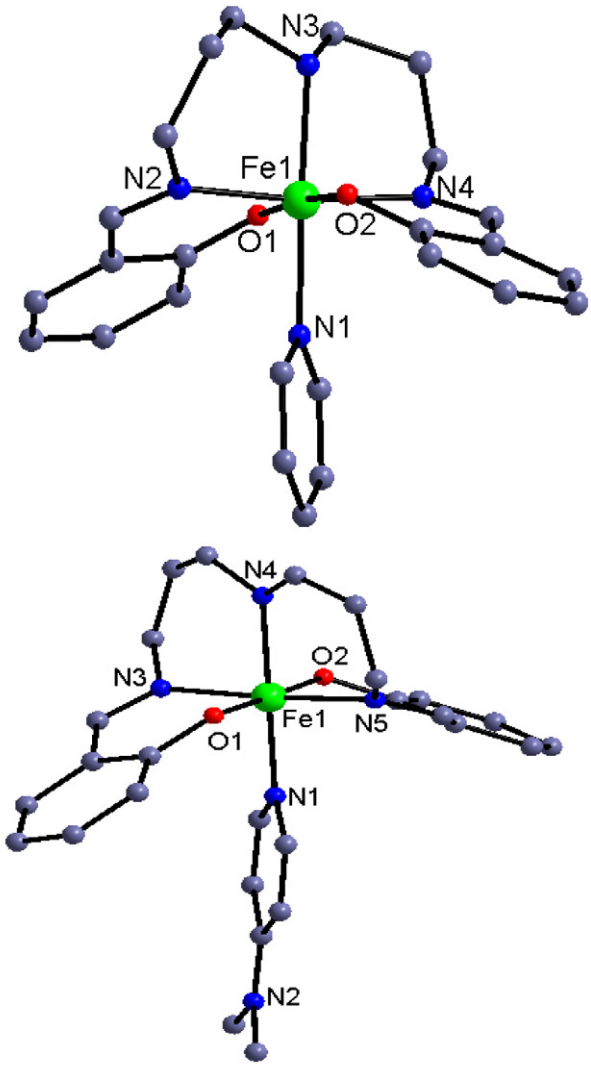

Figure 4. The cationic mononuclear structure of complexes **4** (top) and **5** (bottom). All the H atoms and the balanced anion have been omitted for clarity.

To further confirm the spin transition, the structures of complexes **3** and **4** have been measured at low temperature (120 K). As tabulated in Table 4, the cell volume of these two complexes in the low temperature contracted obviously from 8197.68 to 7932.85 $Å^3$ for **3** and 4208.58 to 4086.34 $Å^3$ for **4**, respectively. The averaged Fe–N and Fe–O bond lengths at low temperature are 1.984(7) **Å**, 1.993(5) **Å**, 1.878(5) Å, 1.867(7) Å, which are conspicuously shorter than the room temperature ones with the values 2.045(7) and 2.099(2) Å, indicating different spin state of the Fe(III) ion in these complexes. The comparatively smaller difference for complex **4** can be attributed to the mixed spin state of Fe(III) ion at room temperature, proved also by the magnetic property (*vide infra*).

3.2 Magnetic Properties of Complexes 1–5.

The temperature dependent magnetic susceptibilities of the five complexes were measured by using the corresponding single crystal with quality about 10–20 mg in the range of 2–300 K under an external magnetic field of 2000 Oe. The room temperature $\chi_m T$ values of complexes **1** and **2** (Figure 5) are 4.78 and 4.29 emu K mol^{-1}, respectively, which are basically consistent with the spin only value 4.75 and 4.375 emu K mol^{-1} for the free low spin Fe(III) and high spin Fe(III) ion or the only high spin Fe(III) ion (the cyanide precursor in complex **2** is diamagnetic), respectively. For complex **1**, the $\chi_m T$ value increases with very low speed and attain the highest peak about 5.23 emu K mol^{-1} with the temperature decreasing to about 10 K, and then decreases at a high speed and reaches the value of about 3.85 emu K mol^{-1} at 2 K. The $\chi_m T$-T change tendency can preliminarily confirm the ferromagnetic coupling between the high spin and low spin Fe(III) ion through the cyanide bridge. For complex **2**, with temperature decreasing from 300 K, the $\chi_m T$ value keeps always constant until the sample is cooled to about 20 K, and since then the $\chi_m T$ began to decrease obviously and reaches the lowest value about 3.23 emu K mol^{-1} at 2 K, demonstrating the always high spin state of the Fe(III) ion in this complex.

The ferromagnetic coupling observed in complex **1** can be understood by the orthogonality between the t_{2g} and e_g magnetic orbital of high and low spin Fe(III) ions through the bridging cyanide group. On the basis of the binuclear model, the magnetic susceptibility of complex **1** can be fitted accordingly by the following expression derived from the exchange spin Hamiltonian $\hat{H} = -J\hat{S}_{Fe(HS)}\hat{S}_{Fe(LS)}$:

$$\chi_m = \frac{Ng^2\beta^2}{kT} \cdot \frac{10\exp(-3J/kT)+28}{5\exp(-3J/kT)+7} \quad (1)$$

By using the above model, the susceptibility over the temperature range of 10–300 K was simulated, giving the best-fit parameters J = 1.47(1), g = 2.01(2), $R = \Sigma(c_{obsd}T$ –

$c_{cald}T)^2/\Sigma(c_{obsd}T)^2 = 4.37 \times 10^{-5}$. The small positive *J* value indicates also the ferromagnetic interaction in complex **1**. To further confirm the magnetic coupling nature in complex **1**, the field-dependent magnetization measured up to 50 kOe at 2 K was carried out. The experimental M-H curve (Inset of Figure 5) are basically consistent with the calculated Brillouin function corresponding to the ferromagnetic coupled low spin Fe(III) (S = 1/2) ion and high spin Fe(III) (S = 5/2) ion with $g = 2.0$ at 2 K. The saturated magnetization value is about 5.89 *N*β, which is very close to the expected theoretical value (6.0 *N*β), indicating further the existed overall weak ferromagnetic interactions between the adjacent Fe(III) ions.

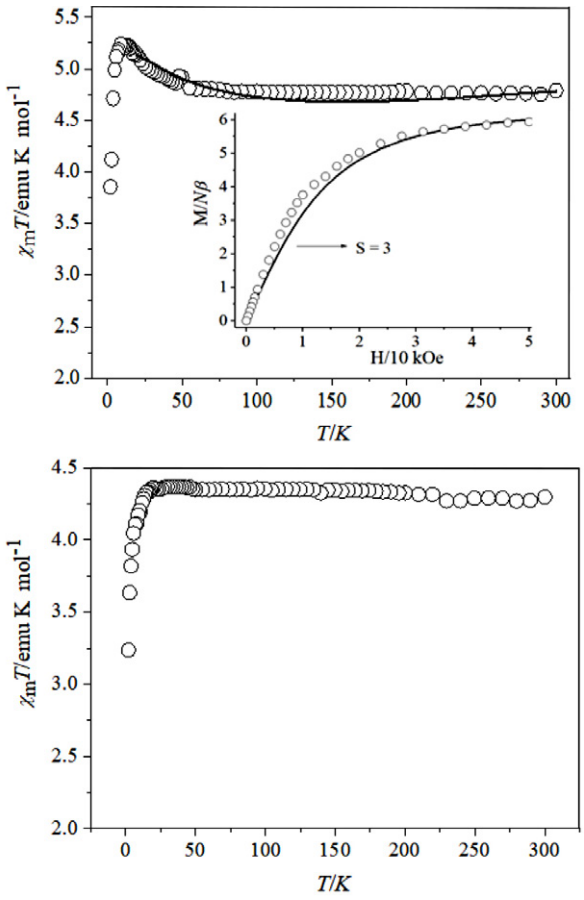

Figure 5. Temperature dependence of χ_mT of **1** (top) and **2**(bottom). Inset: Field dependence of magnetization at 2 K of complex **1**(the solid Brillouin curve is the ferromagnetic coupled one low spin Fe(III) ion and one high spin Fe(III) ion for complex **1**).

The $\chi_m T$-*T* curves of complexes **3-5** are shown in Figure 6 and Figure S1 (Support Information). The room temperature $\chi_m T$ value for complex **3** is about 7.4 emu K mol^{-1}, indicating the two Fe(III) ions bridged by the bipyridine ligand are with almost complete high spin state. For complexes **4** and **5**, the $\chi_m T$ values at 300 K are only 1.82 and 1.41 emu K mol^{-1}, providing clear information that the stable high spin state of the Fe(III) ions in these two complexes outclass the room temperature. With the temperature lowering, the $\chi_m T$ for all the three complexes decreases with a rapid speed to about 1.33, 0.61 and 0.55 cm^3 K mol^{-1} at about 115, 170 and 200 K, respectively, showing the occurrence of a gradually almost complete spin transition. After that, the $\chi_m T$ values keep almost constant with the temperature cooling to 2 K, indicating the stable low spin state at low temperature for these three complexes. Such types of the $\chi_m T$-*T* change tendency can also be found in the reported examples based on the similar pentadentate Schiff base Fe(III) precursor and pyridine-like ligands.

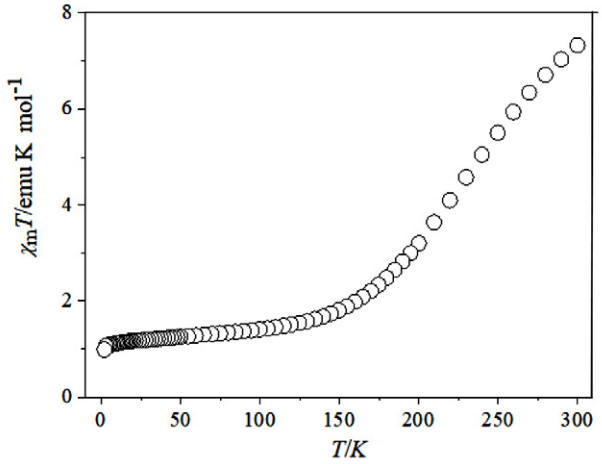

Figure 6. Temperature dependence of χ_mT of **3**

4. Conclusion

In summary, for the purpose of preparation of Fe(II)-based spin crossover molecular magnetic materials, the reactions of pentadentate Schiff base based Fe(III) compounds with the *trans*-dicyanometallates or the pyridine-type ligands were investigated, leading to cyano precursor or 4,4'-bipy bridged binuclear and pyridine coordinated mononuclear complexes. The study over the temperature dependence of the magnetic susceptibility and the field-dependent magnetization revealed the ferromagnetic coupling in cyanide-bridged Fe(III)(low spin)-Fe(III)(high spin) complex. For the pyridine-like ligand involved mono- or binuclear Fe(III) complexes, the thermo-induced gradual complete spin crossover behavior occurring at different temperatures could be found, revealed the important role of the auxiliary ligand with different coordination fields, which provided meaningful information for the future design of SCO magnetic material.

Acknowledgement

This work was supported by the Natural Science Foundation of China (22171166). All authors disclosed no relevant relationships.

5. References

1. P. Wang, Y. Xu, Q. Lin and M. Lu, *Chem. Soc. Rev.* **2018,** *20*, 7522–7538. **DOI:**10.1039/C8CS00372F
2. P. He, J. G. Zhang, X. Yin, J. T. Wu, L. Wu, Z. N. Zhou and T. L. Zhang, *Chem. Eur. J.* **2016**, *22*, 7670–7685. **DOI:**10.1002/chem.201600257
3. D. K. Mahapatra, S. K. Bharti, V. Asati and S. K. Singh, *Eur. J. Med. Chem.* **2019**, *174*, 142–158. **DOI:**10.1016/j.ejmech.2019.04.032
4. J. K. Sun, X. D. Yang, G. Y. Yang and J. Zhang, *Coord. Chem. Rev.* **2019**, *378*, 533–560. **DOI:**10.1016/j.ccr.2017.10.029
5. J. G. Haasnoot, *Coord. Chem. Rev.* **2000**, *200*, 131–185. **DOI:**10.1016/S0010-8545(00)00266-6
6. G. N. Liu, W. J. Zhu, Y. N. Chu and C. Li, *Inorg. Chim. Acta.* **2015**, *425*, 28–35. **DOI:**10.1016/j.ica.2014.10.024
7. R. Mukherjee, *Coord. Chem. Rev.* **2000**, *203*, 151–218. **DOI:**10.1016/S0010-8545(99)00144-7
8. M. B. Bushuev, Y. V. Gatilov, V. P. Krivopalov and O. P. Shkurko, *Inorg. Chim. Acta.* **2015**, *425*, 182–188. **DOI:**10.1016/j.ica.2014.10.017
9. C. Gao, J. Wang, H. Xu and Y. Xiong, *Chem. Soc. Rev.* **2017**, *46*, 2799–2823. **DOI:**10.1039/C6CS00727A
10. R. D. Antonio, J. M. Antonio, C. Joan, R. José, D. C. L. Duane and C. Enrique, *Dalton Trans.* **2009**, *32*, 6335–6344.
11. J. S. Miller and D. Gatteschi, *Chem. Soc. Rev.* **2011**, *40*, 3065–3066. **DOI:**10.1039/c1cs90019f
12. T. K. Ekanayaka, G. Hao, A. Mosey, A. S. Dale, X. Jiang, A. J. Yost, K. R. Sapkota, G. T. Wang, J. Zhang, A. T. N'Diaye, A. Marshall, R. Cheng, A. Naeemi, X. Xu and P. A. Dowben, *Magnetochemistry.* **2021**, *7*, 37. **DOI:**10.3390/magnetochemistry7030037
13. Y. Chen, J. G. Ma, J. J. Zhang, W. Shi, P. Cheng, D. Z. Liao and S. P. Yan, *Chem. Commun.* **2010**, *46*, 5073–5075. **DOI:**10.1039/b927191k
14. M.-L. Hu, A. Morsali and L. Aboutorabi, *Coord. Chem. Rev.* **2011**, *255*, 2821–2859. **DOI:**10.1016/j.ccr.2011.05.019
15. B. Brizet, A. Eggenspiller, C. P. Gros, J. M. Barbe, C. Goze, F. Denat and P. D. Harvey, *J. Org. Chem.* **2012**, *77*, 3646–3650. **DOI:**10.1021/jo3000833
16. D. Tanaka, N. Aketa, H. Tanaka, T. Tamaki, T. Inose, T. Akai, H. Toyama, O. Sakata, H. Tajiri and T. Ogawa, *Chem. Commun.* **2014**, *50*, 10074–10077. **DOI:**10.1039/C4CC04123B
17. M. A. Halcrow, *Chem. Lett.* **2014**, *43*, 1178–1188. **DOI:**10.1246/cl.140464
18. A. Bousseksou, G. Molnár, L. Salmon and W. Nicolazzi, *Chem. Soc. Rev.* **2011**, *40*, 3313–3335. **DOI:**10.1039/c1cs15042a
19. A. Tissot, X. Kesse, S. Giannopoulou, I. Stenger, L. Binet, E. Rivière and C. Serre, *Chem. Commun.* **2019**, *55*, 194–197. **DOI:**10.1039/C8CC07573E
20. D. Gao, Y. Liu, B. Miao, C. Wei, J. G. Ma, P. Cheng and G. M. Yang, *Inorg. Chem.* **2018**, *57*, 12475–12479. **DOI:**10.1021/acs.inorgchem.8b02408
21. A. B. Gaspar, V. Ksenofontov, M. Seredyuk and P. Gütlich, *Coord Chem. Rev.* **2005**, *249*, 2661–2676. **DOI:**10.1016/j.ccr.2005.04.028
22. B. Benaicha, K. Van. Do, A. Yangui, A. Yangui, N. Pittala, A. Lusson, M. Sy, G. Bouchez, H. Fourati, C. J. Gómez-García, S. Triki and K. Boukheddaden, *Chem. Sci.* **2019**, *10*, 6791–6798. **DOI:**10.1039/C9SC02331C
23. R. Ohtani and S. Hayami, *Chem. Eur. J.* **2017**, *23*, 2236–2248. **DOI:**10.1002/chem.201601880
24. Z. P. Ni, J. L. Liu, M. N. Hoque, W. Liu, J. Y. Li, Y. C. Chen and M. L. Tong, *Coord. Chem. Rev.* **2017**, *335*, 28–43. **DOI:**10.1016/j.ccr.2016.12.002
25. J. L. Wang, Q. Liu, Y. S. Meng, X. Liu, H. Zheng, Q. Shi, C. Y. Duan and T. Liu, *Chem. Sci.* **2018**, *9*, 2892–2897. **DOI:**10.1039/C7SC05221A
26. S. Soleymani-Babadi, A. Beheshti, M. Bahrani-Pour, P. Mayer, H. Motamedi, D. Trzybinski and K. Wozniak, *Cryst. Growth. Des.* **2019**, *19*, 4934–4948. **DOI:**10.1021/acs.cgd.9b00038
27. A. Beheshti, E. S. M. Fard, M. Kubicki, P. Mayer, C. T. Abrahams and S. E. Razatofighi, *Cryst Eng Comm.* **2019**, *21*, 251–262. **DOI:**10.1039/C8CE01348A
28. M. A. Halcrow, *Chem. Soc. Rev.* **2011**, *40*, 4119–4142. **DOI:**10.1039/c1cs15046d
29. I. Nemec, R. Boča, R. Herchel, Z. Trávníček, M. Gembický and W. Linert, *Monats. Chem*. **2009**, *140*, 815–828. **DOI:**10.1007/s00706-008-0096-0
30. Y. Komatsumaru, M. Nakaya, F. Kobayashi, R. Ohtani, M. Nakamura, L. F. Lindoy and S. Hayami, *Z. Anorg. Allge. Chem.* **2018**, *644*, 729–734. **DOI:**10.1002/zaac.201800087
31. S. Vela, M. Fumanal, J. Cirera and J. Ribas-Arino, *Phys. Chem. Chem. Phys.* **2020**, *22*, 4938–4945. **DOI:**10.1039/D0CP00162G
32. T. Fujinami, K. Nishi, R. Kitashima, K. Murakami, N. Matsumoto, S. Iijima and K. Toriumi, *Inorg. Chim. Acta*. **2011**, *376*, 136–143. **DOI:**10.1016/j.ica.2011.06.004
33. D. J. Harding, P. Harding and W. Phonsri, *Coord. Chem. Rev*. **2016**, *313*, 38–61. **DOI:**10.1016/j.ccr.2016.01.006
34. S. Mukherjee, T. Weyhermüller, E. Bill, K. Wieghardt and P. Chaudhuri, *Inorg. Chem.* **2005**, *44*, 7099–7108. **DOI:**10.1021/ic050885l
35. H. Chun, C. N. Verani, P. Chaudhuri, E. Bothe, E. Bill, T. Weyhermüller and K. Wieghardt, *Inorg. Chem.* **2001**, *40*, 4157–4166. **DOI:**10.1021/ic010106a
36. M. Arai, W. Kosaka, T. Matsuda and S. Ohkoshi, *Chem. Int. Ed.* **2008**, *47*, 6885–6887. **DOI:**10.1002/anie.200802266
37. K. Tanimura, R. Kitashima, N. Brefuel, M. Nakamura, N. Matsumoto, S. Shova and J. P. Tuchagues, *Bull. Chem. Soc. Jpn.* **2005**, *78*, 1279–1282. **DOI:**10.1246/bcsj.78.1279
38. R. Kitashima, S. Imatomi, M. Yamada, N. Matsumoto and Y. Maeda, *Chem. Lett*. **2005**, *34*, 1388–1389. **DOI:**10.1246/cl.2005.1388
39. W. Phonsri, L. C. Darveniza, S. R. Batten and K. S. Murray, *Inorganics.* **2017**, *5*, 51. **DOI:**10.3390/inorganics5030051
40. W. Phonsri, D. Macedo, B. A. Lewis, D. F. Wain and K. S. Murray, *Magnetochemistry*. **2019**, *5*, 37. **DOI:**10.3390/magnetochemistry5020037
41. W. Phonsri, B. A. I. Lewis, G. N. L Jameson and K. S. Murray, *Chem. Commun.* **2019**, *55*, 14031–14034.

DOI:10.1039/C9CC07416C

42. O. I. Kucheriv, I. O. Fritsky and I. A. Gural'skiy, *Inorg. Chim. Acta.* **2021**, *521*, 120303. **DOI:**10.1016/j.ica.2021.120303
43. Z. H. Ni, L. F. Zhang, C. H. Ge, A. L. Cui,H. Z. Kou and J. Jiang, *Transit. Metal. Chem.* **2008**, *11*, 94–96. **DOI:**10.1016/j.inoche.2007.10.017
44. D. Zhang and H. Zhang, *Polyhedron.* **2015**, *100*, 36–42. **DOI:**10.1016/j.poly.2015.07.024
45. D. Zhang, L. Kong, P. Wang and X. Chen, *Synth. Ynth. React. Inorg. M.* **2016**, *46*, 828–831.

DOI:10.1080/15533174.2014.989597

46. J. Shi, Q. Meng, C. Xue, Q. Liu and D. Zhang, *Transit. Metal. Chem.* **2018**, *43*, 45–52. **DOI:**10.1007/s11243-017-0192-2
47. Z. H. Ni, H. Z. Kou, L. F. Zhang, C. Ge, R. J. Wang and A. L. Cui, *J. Chem. Crystallog.* **2006**, *36*, 465–472.
48. D. Zhang, P. Wang, Z. Zhao and X. Chen, *J. Coord. Chem.* **2014**, *67*, 1664–1672. **DOI:**10.1080/00958972.2014.918266
49. R. Boča, Y. Fukuda, M. Gembický, R. Herchel, R. Jaroščiak, W. Linert, F. Renz and J. Yuzurihara, *Chem. Phys. Lett.* **2000**, *325*, 411–419. **DOI:**10.1016/S0009-2614(00)00701-6
50. R. Kitashima, S. Imatomi, M. Yamada, N. Matsumoto and Y. Maeda, *Chem. Lett.* **2005**, *34*, 1388–1389. **DOI:**10.1246/cl.2005.1388
51. N. Matsumoto, S. Ohta, C. Yoshimura, A. Ohyoshi, S. Kohata, H. Okawa and Y. Maeda, *J. Chem. Soc. Dalton Trans.* **1985**, *12*, 2575–2584. **DOI:**10.1039/dt9850002575
52. H. Z. Kou, Z. H. Ni, C. M. Liu, D. Q. Zhang and A. L. Cui, *New J. Chem.* **2009**, *33*, 2296–2299. **DOI:**10.1039/b9nj00316a
53. T. Senapati, C. Pichon, R. Ababei, C. Mathonièr and R. Clérac, *Inorg. Chem*. **2012**, *51*, 3796–3812. **DOI:**10.1021/ic2027708

Povzetek

Serija dvo- ali enojedernih heksakoordiniranih kompleksov železa(III), $[Fe(L)][Fe(bpb)(CN)_2]\cdot CH_3OH\cdot 0.5H_2O$ (**1**), $[Fe(L)][Co(bpb)(CN)_2]\cdot CH_3OH$ (**2**) $[(Fe(L))_2(4,4'\text{-bipy})](BPh_4)_2$ (**3**), $[Fe(L)(py)](BPh_4)$ (**4**) in $[Fe(L)(dmap)](BPh_4)$ (**5**) (bpb = 1,2-bis(piridin-2-karboksamido)benzenat, L = *N*,*N*'-bis(2-hidroksibenziliden)-1, 7-diamino-4-azaheptan, dmap = 4-dimetilaminopiridin), je bila pripravljena iz **želez**ovega(III) kompleksa s pentadentatno Schiffovo bazo kot prekurzorjem ter okarakterizirana z elementno analizo, IR in rentgensko difrakcijo. Strukturna analiza monokristalov je razkrila nevtralno cianidno vezano dvojedrno zvrst za kompleksa **1** in **2** ter kationsko dvo- ali enojedrno strukturo za komplekse **3**–**5** s pozitivnim nabojem ter BPh_4^- protiionom. Eksperimenti in teoretične simulacije magnetnih lastnosti razkrijejo feromagnetno sklopitev med Fe(III) ioni, ki jih povezuje cianidna skupina v kompleksu **1**, in visokospinsko stanje Fe(III) iona, koordiniranega z ligandom Schiffove baze v kompleksih **1** in **2**. Raziskava magnetne susceptibilnosti kompleksov **3**–**5** v odvisnosti od temperature je pokazala, da se pri približno 115, 170 in 200 K pojavi toplotno-induciran popoln spinski prehod.